Time Reversal of Bose-Einstein Condensates

J. Martin, B. Georgeot, and D. L. Shepelyansky
Laboratoire de Physique Théorique, Université de Toulouse III, CNRS, 31062 Toulouse, France
(Received 22 April 2008; published 13 August 2008)

Using Gross-Pitaevskii equation, we study the time reversibility of Bose-Einstein condensates (BEC) in kicked optical lattices, showing that in the regime of quantum chaos, the dynamics can be inverted from explosion to collapse. The accuracy of time reversal decreases with the increase of atom interactions in BEC, until it is completely lost. Surprisingly, quantum chaos helps to restore time reversibility. These predictions can be tested with existing experimental setups.

DOI: 10.1103/PhysRevLett.101.074102 PACS numbers: 05.45.Mt, 03.75.−b, 37.10.Jk, 67.85.Hj

In recent years, remarkable progress has been made in the manipulation and control of the dynamics of BEC in optical lattices (see, e.g., the review [1]). In such systems, the velocity spread is very small. This allows to perform very precise investigations of the kicked rotator, known as a paradigm of quantum and classical chaos [2]. As a result, high order quantum resonances were recently observed experimentally [3], and various nontrivial effects in the kicked rotator dynamics were probed [4,5]. It should be stressed that in BEC, the interactions between atoms are of crucial importance, in contrast with other implementations of the kicked rotator with cold atoms [6–9], where such interactions are negligible. Recently, a method of time reversal for atomic matter waves has been proposed for the kicked rotator dynamics of noninteracting atoms [10]. This method also allows to realize effective cooling of the atoms by a few orders of magnitude. The problem of time reversal of dynamical motion of atoms originates from the famous dispute between Boltzmann and Loschmidt on the origin of irreversible statistical behavior in time reversible systems [11,12]. The results obtained in [10] showed that the quantum dynamics of noninteracting atoms can be reversed in time even if the corresponding classical dynamics is practically irreversible due to dynamical chaos [13,14]. The investigation of the effect of interactions on time reversibility is of prime importance, since the original dispute between Boltzmann and Loschmidt concerned interacting atoms. In this Letter, we study the effects of interactions between atoms in BEC on the time reversal accuracy. We emphasize that interactions bring new elements in the problem of time reversal compared to the case of one particle quantum dynamics [10], acoustic [15], and electromagnetic waves [16].

To describe the BEC dynamics in a kicked optical lattice, we use Gross-Pitaevskii equation (GPE) [17]

$$i\hbar\frac{\partial}{\partial t}\psi = \left(-\frac{\hbar^2}{2m}\frac{\partial^2}{\partial x^2} - g|\psi|^2 + k\cos(\kappa x)\delta_T(t)\right)\psi \quad (1)$$

where the first two terms on the r.h.s. correspond to the usual GPE, and the last term represents the effect of the optical lattice of period $\lambda = 2\pi/\kappa$, with $\delta_T(t)$ being a periodic delta-function with period T. The interaction between atoms is quantified by the nonlinear parameter $g = Ng_{1D}$ where N is the number of atoms in the condensate and $g_{1D} = -2a_0\hbar\omega_\perp$ is the effective 1D coupling constant, $\omega_\perp$ being the radial trap frequency and a_0 the 3D scattering length. Here, $\psi(x, t)$ is normalized to one. In the following, we choose units such that $\hbar = m = \kappa = 1$so that the momentum of atoms is measured in recoil units; time t is measured in units of T. For $g = 0$, Eq. (1) reduces to the usual kicked rotator model with classical chaos parameter $K = kT$ and effective Planck constant T (see, e.g., [10]). In this case, the time reversal can be done in the way described in [10]: the forward propagation in time is done with $T = 4\pi + \epsilon$ while the backward propagation is performed using $T \rightarrow T' = 4\pi - \epsilon$, with inversion of the sign of k at the moment of time reversal t_r. This procedure allows to perform approximate time reversal (ATR) for atoms with small velocities inside the central recoil cell. This ATR procedure works quite accurately for noninteracting atoms ($g = 0$), but can be significantly affected by the nonlinear interaction [$g \neq 0$ in (1)] encountered in BEC. Indeed, in the regime of strong interactions and BEC size ℓ_s smaller than λ, earlier investigations [18] of the soliton dynamics in GPE with $g > 0$ and periodic boundary conditions have shown that a soliton moves with good accuracy along chaotic classical trajectories of the Chirikov standard map [2]. As a result, even if one performs exact time reversal (ETR), the presence of very small numerical errors completely destroys reversibility due to the instability of chaos. However, here we are mainly interested in the typical regime of BEC experiments where $\ell_s > \lambda$. Our studies show that in this regime, time reversal can be achieved with good accuracy for interactions of moderate strength.

To investigate time reversibility for BEC, we numerically simulated the wave function evolution through (1), using up to $N_s = 2^{23}$ discretized momentum states with $\Delta p = 2.5 \times 10^{-5}$, space discretization $\Delta x = 2\pi/(N_s\Delta p)$, and with up to 4×10^4 integration time steps between two kicks. In this way, we obtain the probability distribution in momentum space $W_p(t) = |\langle p|\psi(t)\rangle|^2$. The results of time

reversal performed by ATR procedure are shown in Fig. 1, for an initial Gaussian distribution in momentum with rms $\sigma = 0.002$ in recoil units (as in the experiment of [3]). After this procedure, the returned wave packet at $t = 2t_r$ becomes clearly squeezed in momentum compared to the initial one. In absence of interactions ($g = 0$), the maximum of the final returned distribution $W_0^f = W_{p=0}(t = 2t_r)$ is equal to the maximum of the initial one $W_0^i = W_{p=0}(t = 0)$ since ATR is exact for $p = 0$ [10]. The increase of the nonlinear parameter g leads to a reduction of the ratio W_0^f/W_0^i until complete destruction of reversibility for $g = 20$. However, the half-width p_L of the returned peak is only weakly affected by g. It should be stressed that at the moment of time reversal t_r, the wave packet is completely destroyed (Fig. 1, left inset), and nevertheless the peak is recreated at $t = 2t_r$ (Fig. 1, right inset). This process looks similar to the observed "Bosenova" explosion induced by the change of sign of the interactions in BEC [19]. In our case, the sign of the interactions is unchanged, but the time reversal allows to invert the explosion which happens during $0 \le t \le t_r$ into a collapse for $t_r < t \le 2t_r$. We also note that the ETR procedure ($\psi(x) \to \psi^*(x)$ at $t = t_r$) leads to an almost perfect time reversal of the wave packet, indicating that exponential instability is rather weak for our t_r.

The behavior of W_0^f/W_0^i, shown in Fig. 2, can be approximately described through

$$W_0^f/W_0^i \approx e^{-\Gamma t_r}, \qquad \Gamma = Cg^2\sqrt{\sigma}/D_q, \tag{2}$$

where C is a numerical constant and D_q is the quantum diffusion rate which determines the localization length l of quantum eigenstates in momentum space when $g = 0$: $l = D_q/2$ with $D_q \approx k^2/2$ (see [10] for the exact expression of D_q). Surprisingly enough, the accuracy of time reversal increases when the chaotic diffusion rate D_q increases (see Fig. 2). Qualitatively, this is due to the faster spreading of the wave function in coordinate space that leads to a decrease of the nonlinear term $g|\psi(x,t)|^2$ in (1), making the dynamics closer to the linear case for which $W_0^f = W_0^i$. An estimate for Γ can be obtained assuming that the nonlinear term generates additional corrections $k \to k + a(t)$ in (1), where a randomly varies in time and $a \sim g|\psi|^2 \sim g\sigma/\sqrt{l}$. This relation takes into account the normalization condition ($|\psi|^2/\sigma \sim 1$) and assumes that inhomogeneities in $|\psi(x)|^2$ are smoothed over $l \sim D_q$ localized chaotic eigenstates. With these assumptions, the decay rate of W_0^f/W_0^i is given by the Fermi golden rule $\Gamma \sim |a|^2 \sim g^2\sigma^2/D_q$. Such a consideration assumes that σ remains constant during the dynamics while in fact it increases due to diffusion in momentum that probably leads to the smaller power of σ found numerically (2). These estimates qualitatively explain the surprising result of Fig. 2 which shows that the increase of quantum chaos diffusion D_q improves the time reversal at fixed g.

In addition to the ATR procedure described above, it is possible to perform additionally the inversion of the sign of the interactions g at $t = t_r$. In principle, such an inversion of g can be realized in experiments similar to those of [19]. The numerical data for this case are shown in the inset of Fig. 2. They can be described by the same formula as for

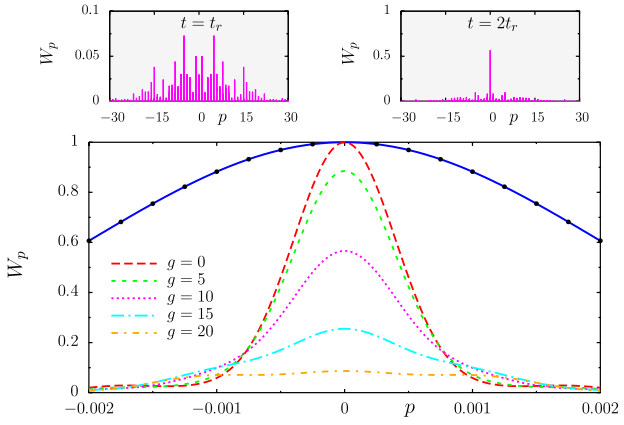

FIG. 1 (color online). Initial (blue/black solid curve) and final return probability distributions W_p obtained by ATR procedure vs momentum p for various nonlinearities g. Insets : probability distribution W_p at $t = t_r = 10$ (left) and final one at $t = t_f = 2t_r$ (right) on a larger scale for $g = 10$. All probability distributions are scaled by their value at $p = 0$, $t = 0$. Initial state is a Gaussian packet with rms $\sigma = 0.002$. Here, $k = 4.5$, $T = 4\pi + \epsilon$ for $0 \le t \le t_r$ and $T' = 4\pi - \epsilon$ for $t_r < t \le 2t_r$ with $\epsilon = 2$ and $t_r = 10$. Black dots correspond to the wave function after ETR procedure.

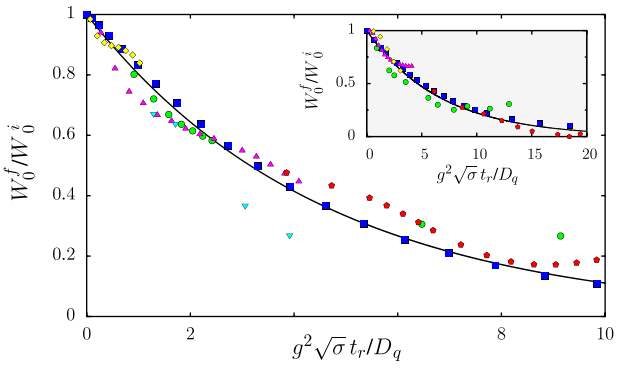

FIG. 2 (color online). Ratio of final to initial probabilities at $p = 0$ as a function of $g^2\sqrt{\sigma}t_r/D_q$. Symbols mark the numerical data for: $k = 4.5$, $\sigma = 0.002$, $t_r = 10$ ($0 \le g \le 20$, blue squares); $k = 8$, $g = 10$, $t_r = 10$ ($0.002 \le \sigma \le 0.2$, green circles); $k = 4.5$, $g = 10$, $\sigma = 0.002$ ($1 \le t_r \le 15$, magenta triangles); $g = 10$, $\sigma = 0.002$, $t_r = 10$ ($4 \le k \le 9$, cyan reversed triangles); $k = 4.5$, $g = 10$ ($g = 15$ for the inset), $t_r = 10$ ($0.002 \le \sigma \le 0.026$, red pentagons); $k = 4.5$, $g = 5$ ($g = 15$ for the inset), $\sigma = 0.002$ ($1 \le t_r \le 15$, yellow diamonds); the curve shows the dependence (2) with $C = 0.22$. Inset : same ratio but for a change of sign of g during the reversed evolution, the curve has $C = 0.15$.

the case of unchanged g, but with a smaller numerical constant C. The relatively small difference between the two cases indicates that the main mechanism of time reversal destruction is related to transitions to other momentum states induced by the nonlinear interaction.

The time reversal leads to a squeezing of the wave packet in momentum space near $p = 0$, that can be interpreted as an effective Loschmidt cooling [10]. The effects of interactions on this cooling process are analyzed in Fig. 3. The temperature T_f of the returned atoms can be defined as the temperature of those atoms with momentum in the interval $[-2p_L, 2p_L]$ at $t = 2t_r$ (see [10]). For $g = 0$, the ratio T_f/T_0 of final to initial temperatures drops significantly with k. At small $g = 0.5$, the ratio remains essentially unchanged for all values of k considered. In contrast, for stronger nonlinearity ($g = 10$), there is no cooling at low values of $k \leq 3$, but for strong chaos with $k > 3$, cooling reappears and becomes very close to the case $g = 0$ at large k values. Thus, strong quantum chaos surprisingly enhances the cooling of BEC. This result is the consequence of relation (2), according to which the return probability becomes larger and larger with the increase of the quantum diffusion rate $D_q \approx k^2/2$.

The results presented in Figs. 1–3 show that time reversal can be performed for BEC through the ATR procedure even in the presence of strong interactions. The cooling mechanism works also in the presence of these interactions, provided quantum chaos is sufficiently strong.

Up to now, we have discussed the case of BEC with $\ell_s \gg \lambda$. It is also interesting to analyze the opposite regime $\ell_s < \lambda$ with the initial soliton distribution

$$\psi(x,t) = \frac{\sqrt{g}}{2} \frac{\exp[ip_0(x - x_0 - p_0 t/2) + ig^2 t/8]}{\cosh[\frac{g}{2}(x - x_0 - p_0 t)]}. \quad (3)$$

For $k = 0$, this is the exact solution of Eq. (1), which describes the propagation of a soliton with constant velocity p_0 [20]. At moderate values of k, the shape of the soliton is only slightly perturbed, and its center follows the dynamics described by the Chirikov standard map [18]: $\bar{p}_0 = p_0 + k \sin x_0$; $\bar{x}_0 = x_0 + \bar{p}_0 T$, where bars denote the values of the soliton position and velocity after a kick iteration. In the chaotic regime with $K > 1$, the soliton dynamics becomes truly chaotic. Indeed, two solitons with slightly different initial velocities or positions diverge exponentially with time. As a result of this instability, even the ETR procedure does not produce an exact return of the soliton to its initial state, due to the presence of numerical integration errors. This is illustrated in Fig. 4, where the distance in phase space δ between the initial and returned solitons is shown as a function of the time reversal moment t_r. If the initial position of the soliton is taken inside the chaotic domain, δ grows exponentially with t_r as $\delta \sim \exp(\Lambda t_r)$. The numerical fit gives a value of Λ very close to the Kolmogorov-Sinai entropy h of the standard map at the corresponding value of K. For large values of t_r, the difference δ becomes so large that the time reversed soliton is located far away from the initial one, meaning that time reversibility is completely destroyed (Fig. 4, left inset). In contrast, if the soliton starts in the regular domain, the growth of δ remains weak during the whole integration time. In this regime, even for large values of t_r, the values of δ remain small and the soliton returns very close to its initial state (Fig. 4, right inset).

Another way to characterize the stability of the nonlinear wave dynamics described by Eq. (1) is to study the behavior of the fidelity defined as $f(t) = |\langle \psi_1(t) | \psi_2(t) \rangle|^2$, where ψ_1 and ψ_2 are two solitons with slightly different initial conditions. It is important to note that for $g = 0$, the function $f(t)$ is independent of t; thus, variation with time appears only due to nonlinear effects. In a certain sense, this quantity can be considered as a generalization of the

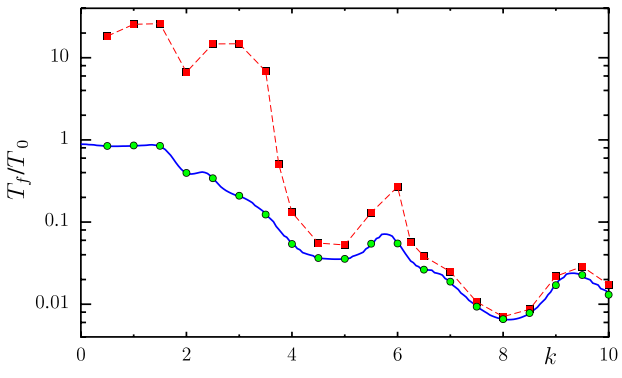

FIG. 3 (color online). Loschmidt cooling of time reversed BEC atoms characterized by the ratio of final T_f and initial T_0 temperatures as a function of k for an initial Gaussian momentum distribution with rms $\sigma = 0.002$ and $g = 0$ (solid curve), $g = 0.5$ (green/gray circles), and $g = 10$ (red/black squares). Here, $t_r = 10$ and $\epsilon = 2$.

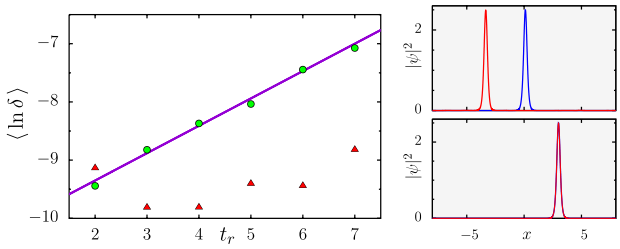

FIG. 4 (color online). Left panel: phase space distance $\delta = \sqrt{\delta x^2 + \delta p^2}$ between the initial soliton and its time reversed image obtained by ETR ($\psi(x) \rightarrow \psi^*(x)$) vs t_r for $k = 1$, $T = 2$, and $g = 10$; symbols show numerical data averaged over 50 trajectories inside the chaotic (green circles) and regular (red triangles) domains. The solid line shows the linear fit $\langle \ln \delta \rangle = 0.47 t_r - 10.29$. The slope is close to the Kolmogorov-Sinai entropy $h \approx 0.45$ at $K = kT = 2$. Right panels: soliton at initial time $t = 0$ (blue/black) and final time $t = 2t_r$ (red/ gray) with $t_r = 40$ for initial conditions inside the chaotic domain (top) and regular domain (bottom, initial, and final solitons are superimposed).

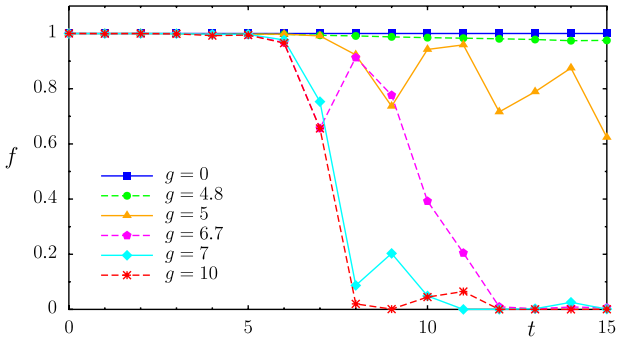

FIG. 5 (color online). Fidelity of two solitons with close initial conditions vs time t for $k = 1$, $T = 2$ and different nonlinearities. The initial states are solitons (3) with $g = 10$ and initial conditions $(x_0, p_0) = (0.5, 1.25)$ and $(x_0', p_0') = (0.5, 1.255)$ inside the chaotic domain.

usual fidelity [21] discussed for the Schrödinger evolution to the case of nonlinear evolution given by GPE. The dependence of f on time is shown in Fig. 5 for different values of the nonlinear parameter g. For small values of g, the function is almost constant on the considered time interval, while for large values of g, it drops quickly to almost zero after a logarithmically short time scale corresponding to the separation of the two solitons. These two qualitatively different behaviors can be understood as follows. For relatively weak nonlinearity, $f(t) \sim \exp(-\Gamma t)$ with $\Gamma \propto g^2$ [see Eq. (2)] that corresponds to the usual Fermi golden rule regime of the fidelity decay in linear quantum systems with perturbation [21]. For stronger g, we enter the regime where nonlinear wave packets move like chaotic individual particles which leads to an abrupt drop of fidelity as soon as the separation becomes larger than the size of the wave packets. In this regime, $\ell_s < \lambda$ and time reversal is destroyed. In the opposite limit $\ell_s > \lambda$ shown in Fig. 1, the time reversal can be maintained at moderate values of g. The transition between these two regimes is rather nontrivial and requires further investigations.

The results of Figs. 4 and 5 show that the soliton dynamics described by GPE (1) is truly chaotic. This leads to the destruction of time reversibility induced by exponential growth of small perturbations. However, the real BEC is a quantum object with a mass proportional to the number N of atoms. Thus, it has effective $\hbar_{\rm eff} \propto 1/\sqrt{N}$, and since the Ehrenfest time t_E for chaotic dynamics depends only logarithmically on $\hbar$ [2,21], this time remains rather short $t_E \sim |\ln \hbar_{\rm eff}|/h \sim (\ln N)/2h$. Thus, for the parameters of Fig. 4 with $N = 10^5$, we have $t_E \approx 13$, and the quantum BEC should have no exponential instability of motion on a larger time scale. Hence, in the time reversal procedure, the real quantum BEC remains stable and reversible contrary to the BEC described by GPE. We think that the resolution of this paradox relies on the absence of second quantization in GPE that makes the soliton dynamics essentially classical.

The dimensionless nonlinear parameter is $g = -Na_0\lambda/4\pi l_\perp^2$, where $l_\perp = \sqrt{\hbar/m\omega_\perp}$. Values of $g \approx 0.1$ have been achieved with a radial frequency ≈ 800 Hz and $N \approx 5000 \approx N_{\rm max} = l_\perp/|a_0|$[22]. This value can be further increased up to $g \approx 10$ by increasing $\omega_\perp$ (e.g., to 20 kHz [23]) and increasing λ using a CO_2-laser [24] or crossed laser beams. Thus, experimental setups similar to [3–5,22] can test the fundamental question of BEC time reversal discussed here.

We thank CalMiP for access to their supercomputers and the French ANR (Project INFOSYSQQ) and the EC Project EuroSQIP for support.

[1] O. Morsch and M. Oberthaler, Rev. Mod. Phys. **78**, 179 (2006).
[2] B. V. Chirikov, Phys. Rep. **52**, 263 (1979); B. V. Chirikov *et al.*, Sov. Sci. Rev., Sect. C **2**, 209 (1981); Physica D (Amsterdam) **33**, 77 (1988); B. Chirikov and D. Shepelyansky, Scholarpedia **3**, No. (3), 3550 (2008).
[3] C. Ryu *et al.*, Phys. Rev. Lett. **96**, 160403 (2006).
[4] G. Behinaein *et al.*, Phys. Rev. Lett. **97**, 244101 (2006).
[5] S. A. Wayper *et al.*, Europhys. Lett. **79**, 60006 (2007).
[6] F. L. Moore *et al.*, Phys. Rev. Lett. **75**, 4598 (1995).
[7] H. Ammann *et al.*, Phys. Rev. Lett. **80**, 4111 (1998).
[8] S. Schlunk *et al.*, Phys. Rev. Lett. **90**, 124102 (2003).
[9] J. Chabé *et al.*, arXiv:0709.4320.
[10] J. Martin *et al.*, Phys. Rev. Lett. **100**, 044106 (2008).
[11] J. Loschmidt, Sitzungsberichte der Akademie der Wissenschaften, Wien, II **73**, 128 (1876).
[12] L. Boltzmann, Sitzungsberichte der Akademie der Wissenschaften, Wien, II **75**, 67 (1877).
[13] I. P. Kornfeld *et al.*, *Ergodic Theory* (Springer, N.Y., 1982).
[14] A. Lichtenberg and M. Lieberman, *Regular and Chaotic Dynamics* (Springer, N.Y., 1992).
[15] A. Derode *et al.*, Phys. Rev. Lett. **75**, 4206 (1995); J. de Rosny *et al.*, *ibid.* **84**, 1693 (2000).
[16] G. Lerosey *et al.*, Phys. Rev. Lett. **92**, 193904 (2004); Science **315**, 1120 (2007).
[17] F. Dalfovo *et al.*, Rev. Mod. Phys. **71**, 463 (1999).
[18] F. Benvenuto *et al.*, Phys. Rev. A **44**, R3423 (1991).
[19] E. A. Donley *et al.*, Nature (London) **412**, 295 (2001).
[20] V. E. Zakharov and A. B. Shabat, Zh. Eksp. Teor. Fiz. **61**, 118 (1971) [Sov. Phys. JETP **34**, 62 (1972)].
[21] T. Gorin *et al.*, Phys. Rep. **435**, 33 (2006).
[22] K. E. Strecker *et al.*, Nature (London) **417**, 150 (2002).
[23] I. Llorente-Garcia *et al.*, J. Phys. Conf. Ser. **19**, 70 (2005).
[24] S. Friebel *et al.*, Phys. Rev. A **57**, R20 (1998).